EBioMedicine 61 (2020) 103031

Contents lists available at ScienceDirect

EBioMedicine

journal homepage: www.elsevier.com/locate/ebiom

Research paper

A liquid biopsy for detecting circulating mesothelial precursor cells: A new biomarker for diagnosis and prognosis in mesothelioma

Bill T.V. Duong[a,1], Licun Wu[b,1], Brenda J. Green[c], Fatemeh Bavaghar-Zaeimi[b,f], Zongjie Wang[c,d], Mahmoud Labib[e], Yuxiao Zhou[e], Fernando J.P. Cantu[e], Thurgaa Jeganathan[e], Sandra Popescu[e], Jennifer Pantea[e], Marc de Perrot[b,f,g,*], Shana O. Kelley[a,c,e,h,*]

[a] Department of Chemistry, University of Toronto, 80 St George St., Toronto, Ontario M5S 3H6, Canada
[b] Latner Thoracic Surgery Research Laboratories, Toronto General Hospital Research Institute, 101 College St., Toronto, Ontario M5G 1L7, Canada
[c] Institute for Biomaterials and Biomedical Engineering, University of Toronto, 164 College St., Toronto, Ontario M5S 3G9, Canada
[d] The Edward S. Rogers Sr. Department of Electrical and Computer Engineering, University of Toronto, 10 King's College Rd., Toronto, Ontario M5S 3G4, Canada
[e] Department of Pharmaceutical Sciences, University of Toronto, 144 College St., Toronto, Ontario M5S 3M2, Canada
[f] Division of Thoracic Surgery, Toronto General Hospital and Princess Margaret Cancer Centre, University Health Network, 200 Elizabeth St., Toronto, Ontario M5G 2C4, Canada
[g] Department of Immunology, University of Toronto, 27 King's College Circle, Toronto, Ontario M5S 1A1, Canada
[h] Department of Biochemistry, University of Toronto, 27 King's College Circle, Toronto, Ontario M5S 1A1, Canada

ARTICLE INFO

Article History:
Received 4 June 2020
Revised 10 September 2020
Accepted 11 September 2020
Available online xxx

Keywords:
Mesothelioma
Liquid biopsy
Mesothelial precursor cells
Diagnostic biomarker
Clinical prognosis
Molecular profiling

ABSTRACT

Background: Malignant pleural mesothelioma (MPM) is an aggressive cancer related to asbestos exposure. Early diagnosis is challenging due to generic symptoms and a lack of biomarkers. We previously demonstrated that mesothelial precursor cells (MPC) characterized by mesothelin (MSLN)+CD90+CD34+ could be implicated in the development of mesothelioma after asbestos exposure. Here, we aimed to determine the clinical significance of detecting MPC in blood for early-stage diagnosis and prognosis of mesothelioma.
Methods: Due to the rarity of MPC in blood, it is challenging to identify this cell population using conventional techniques. Hence, we have developed a microfluidic liquid biopsy platform called MesoFind that utilizes an immunomagnetic, mesothelin capture strategy coupled with immunofluorescence to identify rare populations of cells at high sensitivity and precision. To validate our technique, we compared this approach to flow cytometry for the detection of MPC in murine blood and lavage samples. Upon successful validation of the murine samples, we then proceeded to examine circulating MPC in 23 patients with MPM, 23 asbestos-exposed individuals (ASB), and 10 healthy donors (HD) to evaluate their prognostic and diagnostic value.
Finding: MPC were successfully detected in the blood of murine samples using MesoFind but were undetectable with flow cytometry. Circulating MPC were significantly higher in patients with epithelioid MPM compared to HD and ASB. The MPC subpopulation, MSLN+ and CD90+, were upregulated in ASB compared to HD suggesting an early role in pleural damage from asbestos. The MPC subpopulation, MSLN+ and CD34+, in contrast, were detected in advanced MPM and associated with markers of poor prognosis, suggesting a predominant role during cancer progression.
Interpretation: The identification of circulating MPC presents an attractive solution for screening and early diagnosis of epithelioid mesothelioma. The presence of different subtypes of MPC have a prognostic value that could be of assistance with clinical decisions in patients with MPM.
Funding: Princess Margaret Hospital Foundation Mesothelioma Research Fund, Toronto General & Western Hospital Foundation.

1. Introduction

Malignant pleural mesothelioma (MPM) is an aggressive malignancy that is generally associated with asbestos exposure and is one of the most common forms of occupational cancer. Despite several

* Co-senior authors and corresponding authors at: Division of Thoracic Surgery, Toronto General Hospital, 9N-961, 200 Elizabeth St., Toronto, Ontario M5G 2C4, Canada and Department of Chemistry, University of Toronto, 80 St George St., Toronto, Ontario M5S 3H6, Canada.
E-mail addresses: marc.deperrot@uhn.ca (M. de Perrot), shana.kelley@utoronto.ca (S.O. Kelley).
[1] These authors contributed equally to this work.

https://doi.org/10.1016/j.ebiom.2020.103031

Research in context

Evidence before this study: Malignant pleural mesothelioma is an aggressive malignancy with dismal prognosis. Due to the lack of detectable biomarkers in early development of the disease, most mesothelioma patients are typically diagnosed in advanced stages. Mesothelial precursor cells (MPC) are a heterogeneous population of cells that have recently been identified in early recruitment to inflamed mesothelium. We have previously observed a significant increase in MPC in the lavage of malignant murine models which suggests MPC are a suitable biomarker for early monitoring of mesothelioma. MPC are quite rare in circulation and thus to date, no studies have been able to investigate the clinical utility of detecting MPC in mesothelioma.

Add value of this study: This is the first study to isolate and characterize the molecular profiles of MPC in circulation. This study introduces a microfluidic platform for the detection of MPC with superior sensitivity and specificity when compared to other current blood screening approaches. We have defined several subpopulations of MPC and found correlations with their biomarker expression to various clinical indications.

Implications of all the available evidences: Our study introduces a useful liquid biopsy approach for screening mesothelioma patients that has the potential for earlier diagnosis and more precise prognosis. This study further highlights the role of MPC in early to late stages of mesothelioma development.

recent breakthroughs in mesothelioma treatment[1–3], the therapeutic options are still very limited and often lead to poor patient outcomes [4,5]. Due to its long latency period and the lack of technology for early diagnosis, most patients are diagnosed in advanced stages of the disease [6]. Diagnostic suspicion typically relies on medical imaging techniques such as computerized tomography (CT) and positron emission tomography (PET) with confirmation through invasive surgical biopsy. However, these techniques lack the sensitivity required for early detection [7,8]. It is therefore critical to establish early detection biomarkers to improve treatment and patients' quality of life. An ideal biomarker should have high specificity to mitigate misdiagnosis, high sensitivity to allow for earlier detection, and be readily measurable in the blood to minimize invasive procedures. There are numerous reports detailing blood-based biomarkers such as soluble mesothelin [9–12], fibulin-3 [13–15], and osteopontin [9,16] yet to date, no biomarker has been implemented in the clinic for the early detection of mesothelioma [8,17–21]. Although current blood-based tests have very high sensitivity for detecting mesothelioma, these tests lack the specificity required to distinguish mesothelioma from other diseases. Furthermore, the clinical utility of these biomarkers are limited due to the high heterogeneity found in MPM and the need for the presence of an invasive tumor to release the marker in the circulation [22].

To overcome these challenges, we directed our attention to early biological responses prior to tumor development. It is widely accepted that mesothelioma arises from the persistent damage to the mesothelium, often induced by asbestos, and as a consequence immune cells are recruited for healing and repair [23,24]. The evasion of immune surveillance is therefore vital for tumor development and numerous strategies for evasion have been described [23,25–27] such as the immunosuppressive roles of myeloid-derived suppressor cells [28] and M2-polarized macrophages [29]. In our previous work, we reported several microenvironmental changes in the mesothelium of murine models that occurred soon after asbestos injection. In particular, we observed a considerable elevation in mesothelial precursor cells (MPC) in peritoneal lavage collected from asbestos-exposed mice when compared to a control group [30]. Although the functions of MPC are still under discussion, it is believed that the recruitment of macrophages and free floating mesothelial-like cells (mesothelin+) after tissue damage can contribute to the regeneration of the damaged mesothelium and have a potential role in tumor-promotion [31,32]. Here, we extend the investigation of MPCs and mesothelial precursor-like cells by determining the clinical significance of their detection in the blood for early diagnosis and prognosis in mesothelioma.

Flow cytometry is a powerful technique that allows for the phenotypic characterization and identification of heterogeneous populations of cells. In our preliminary work, we attempted to detect CD34+, CD90+, and mesothelin (MSLN)+ MPC in blood as previously described [30,31] using flow cytometry. Unfortunately, this method lacks the sensitivity and resolution for identifying the low levels of these cells in the blood. Microfluidic methods offer advantages for the detection of rare cells due to their high throughput, sensitivity, and selectivity compared to traditional approaches [33]. Here, we introduce a novel liquid biopsy assay that takes advantage of a microfluidic approach called MesoFind to isolate and analyze MPCs and MPC-like cells as potential diagnostic and prognostic biomarkers. Our group has previously developed numerous microfluidic platforms with a similar approach for the detection of rare and novel biomarkers in various cancers and diseases [33–45]. Our prior strategies generally focused on the detection of circulating tumor cells (CTC); however, the detection of MPCs as a screening approach provides significant advantages over CTC analysis for two reasons: (1) MPCs are more abundant than CTCs and, (2) MPCs are likely overexpressed much earlier in the disease. With these two factors in mind, we demonstrate in this work an effective approach that monitors circulating MPC for early diagnosis and prognosis of the disease through systematic studies of both murine and clinical blood samples.

2. Methods

2.1. Ethics statement

All animal experiments were approved by the Animal Research Ethics Board (REB) at the Toronto General Hospital Research Institute (3399.18). Animal care and experiments were performed in accordance with institutional and Canadian Institute of Health guidelines. All individuals have provided written consent and the protocol was approved by the REB at Princess Margaret Cancer Centre (04-0715 and 19-5858).

2.2. Cell lines and culture

RN5 mouse mesothelioma cells (RRID:CVCL_4Z50) were established and provided by the Marc de Perrot group [30]. RN5, H2052 (CRL-5915, RRID:CVCL_1518, ATCC, USA), and H2452 (CRL-5946, RRID:CVCL_1553, ATCC, USA) were cultured in RPMI-1640 (350-015, Wisent Bioproducts, Canada) supplemented with 10% fetal bovine serum (FBS) (Wisent Bioproducts, Canada). Cells were passaged regularly and collected for downstream analysis when the confluency was approximately 80%.

2.3. Mouse intraperitoneal model

Mice were injected intraperitoneally (i.p.) with either RN5 cells or saline as a control. At designated time points after injection, the mice were sacrificed, and the blood and lavage were collected. The collected samples were then processed through flow cytometry and the microfluidic chip, MesoFind. All animal experiments were approved

Table 1
. Smoking and medical history of healthy donors.

Patient ID	Sex	Smoking		Medical History			
		Smoker Status	Packs/Day	Asthma	Hypertension	Heart Attack	Prior Cancer
HD1	Male	Never		No	No	No	No
HD2	Male	Smoker	1	No	No	No	No
HD3	Female	Never		No	No	No	No
HD4	Male	Never		No	No	No	No
HD5	Female	Never		No	No	No	No
HD6	Male	Never		No	No	No	No
HD7	Male	Never		No	No	No	No
HD8	Male	Never		No	No	No	No
HD9	Female	Never		No	No	No	No
HD10	Male	Never		No	No	No	No

by the Animal Research Ethics Board (REB) at the Toronto General Hospital Research Institute.

2.4. Clinical sample collection

All blood samples were collected in CellSave preservation tubes (7900005, Menarini Silicon Biosystems Inc, USA) and blood analysis was performed within 48 hours. From the cohort of 56 individuals recruited, 10 were healthy volunteers (Table 1), 23 were individuals with known exposure to asbestos (Table 2), and 23 were individuals diagnosed with malignant pleural mesothelioma (Table 3). The inclusion criteria for asbestos-exposed individuals were as follows: (1) age $>$ 30 years old, (2) prior asbestos exposure at least 20 years ago and/or (3) documented pleural plaques from x-ray. The exclusion criteria were the presence of any prior cancer other than non-melanomic skin cancer. Healthy individuals had no known exposure to asbestos and no history of any cancer and other medical condition. All individuals have provided written consent and the protocol was approved by the REB at Princess Margaret Cancer Centre.

2.5. Microfluidic chip fabrication

A combination of stereolithography and soft-lithography techniques were used to generate MesoFind microfluidic devices. Briefly, 3D printed positive molds were fabricated using stereolithography (μMicrofluidics Edition 3D Printer from Creative CADworks, Canada). Polydimethylsiloxane (PDMS) (Dow Corning, USA) was cast onto the positive molds and baked for 2 hours at 70°C to generate negative molds. The negative molds were treated in a saturated detergent solution (Sparkleen, Thermo Fisher Scientific, USA) in 70% ethanol for one hour at room temperature. PDMS was then cast onto the negative molds and again baked for 2 hours at 70°C to generate PDMS positive imprints. The PDMS imprints were peeled and bonded onto thickness #1 glass slides (Ted Pella, USA) using plasma treatment and were then incubated overnight at 100°C. The inlets and outlets were punched and high-purity silicone tubing (McMaster-Carr, USA) was inserted. Tubing connections were sealed with liquid PDMS followed by an hour of baking at 70°C. Chips were flushed with 0.1% Pluronic F-68 (P5556, Sigma-Aldrich, USA) in phosphate buffer saline (PBS) (Wisent Bioproducts, Canada) overnight before usage.

2.6. MesoFind sample preparation

All samples prepared for MesoFind processing were aliquoted into 0.5mL volumes. RN5, H2052, and H2452 cells were harvested from culture and suspended in PBS at a density of 50 cells/mL and 200 cells/mL (supplementary figure 1). Mice lavage samples were counted and diluted to 2000 cells/mL in PBS. Blood samples were collected in CellSave preservation tubes (7900005, Menarini Silicon Biosystems Inc, USA) and aliquoted to 0.5 mL right before MesoFind processing. Surface mesothelin were tagged in the 0.5 mL samples with 1μL of anti-mesothelin biotin (ABIN2584767, Antibodies-Online, USA) in mice and RN5 samples or 1 μL of anti-mesothelin biotin (BS-0300R-BIOTIN, Bioss Antibodies, USA) in H2052, H2452, and clinical blood samples and left for 30 minutes at room temperature. Cells were then conjugated with 10 μL of anti-biotin microbeads (130-105-637, Miltenyi Biotec, USA) at room temperature for another 30 minutes.

2.7. MesoFind assay

After an overnight treatment of 0.1% Pluronic F-68 in PBS, the microfluidic chips were assembled with an array of grade N52 neodymium magnets (D14-N52, K&J Magnetics, USA) placed above and below the chip. The chips were then connected to a syringe pump (Chemyx, USA) and were set to withdraw at 500 μL/h. All following steps were performed on-chip using the syringe pump. The Pluronic F-68 were washed away with 100 μL PBS prior to sample introduction. The whole 0.5mL aliquot of sample conjugated with magnetic microbeads were processed through the chip and washed with 500μL of CliniMACS PBS/EDTA buffer (Miltenyi Biotec, USA). Samples were then fixed with 4% paraformaldehyde (PFA) (F8775, Sigma-Aldrich, USA) in PBS and permeabilized with 0.2% Triton-X-100 (X-100, Sigma-Aldrich, USA) in PBS. Cells were then washed with a solution containing 0.1% Tween 20 (P9416, Sigma-Aldrich, USA) and 1% Bovine Serum Albumin (BSA) (A7906, Sigma-Aldrich, USA) in PBS. The captured cells were then immunostained with 200μL of an antibody cocktail containing either 2mg/mL of anti-CD34 AF488 (bs-8996R-A488, Bioss Antibodies, USA), 2mg/mL of anti-CD90 AF555 (bs-0778R-A555, Bioss Antibodies, USA), and 0.6 mg/mL anti-CD45 APC (17-0451-83, Invitrogen, USA) for mice-related samples or 1mg/mL of anti-CD34 AF488 (ab195013, Abcam, Canada), 0.5mg/mL of anti-CD90 AF555 (bs-10430R-A555, Bioss Antibodies, USA), and 1.2% v/v of anti-CD45 APC (555485, BD Biosciences, USA) for human-related samples. Only the immunostaining step was processed at 200μL/h to ensure adequate staining time. The cells were then washed again with washing buffer and stained with DAPI (R37606, Invitrogen, USA). The microfluidic chips are then disassembled from the syringe pumps and magnets and are ready for analysis. After completing the MesoFind protocol above, the microfluidic chips were scanned using a Nikon Ti-E Eclipse microscope with Andor's Neo sCMOS camera. Fluorescent images were obtained in the channels corresponding to DAPI, AF488, AF555, and APC. The images were then overlaid and converted to TIFF format. Imaris x64 8.1.2 (Bitplane, Switzerland) was used to process the TIFF images. Using the program's spot detection feature, the XY-coordinates of the fluorescent markers were identified and exported to Microsoft Excel (Windows, USA). A script written in Visual Basics for Applications (VBA) (Windows, USA) was used to colocalize fluorescent spots and display the total counts for every combination of fluorescent overlap in Excel.

Table 2
. Characteristics of asbestos-exposed individuals.

Patient ID	Age	Sex	Medical Condition					Asbestos Exposure			Smoking Status		
			Asthma	Pleural Plaques	Hypertension	Chest Pain	Previous Cancer / Illnesses	Asbestos Exposure	Years of Exposure	Type of Asbestos	Smoking Status	Packs/Day	Years Smoked
Asb-0503	69	Female	No	Yes	No	Yes	pneumonia	Indirect	N/A	unknown	Never		
Asb-0483	76	Male	No	Yes	No	No	No	Direct	40	Unknown	Never		
Asb-0691	70	Male	No	No	No	No	pneumonia	Indirect	14	Unknown	Never		
Asb-0854	66	Female	No	No	No	Yes	pneumonia	Direct	32	Unknown	Former Smoker	0.25	30
Asb-0939	65	Male	No	No	No	No	No	Indirect	35	Unknown	Former Smoker	2	17
Asb-0045	74	Male	No	Yes	No	No	No	Direct	38	Unknown	Former Smoker	1.5	2
Asb-0935	76	Male	No	Yes	No	No	Basal skin cancer	Direct	63	Unknown	Former Smoker	1	18
Asb-1343	68	Male	No	No	No	No	No	Direct	42	Unknown	Never		
Asb-0674	81	Male	Yes	No	Yes	Yes	Benign skin tumour / pneumonia	Indirect	39	Unknown	Never		
Asb-1397	64	Male	No	No	No	No	N/A	Direct	34	Unknown	Smoker	1	34
Asb-0137	78	Male	No	No	No	No	No	Indirect	19	Unknown	Former Smoker	1	27
Asb-1121	53	Male	No	No	No	No	No	Direct	30	Unknown	Former Smoker	0.25	10
Asb-1400	65	Male	No	No	Yes	No	No	Direct	33	Amphiboles & Chrysotile	Former Smoker	1	40
Asb-0929	76	Male	No	Yes	No	No	No	Indirect	40	Unknown	Never		
Asb-0067	73	Male	No	Yes	No	No	No	Direct	15	Unknown	Smoker	0.25	14
Asb-0064	84	Male	No	Yes	No	No	No	Indirect	39	Unknown	Never		
Asb-1124	59	Male	Yes	No	No	Yes	COPD	Direct	27	Unknown	Former Smoker	1	40
Asb-0501	73	Male	Yes	Yes	No	Yes	No	Direct	37	Unknown	Former Smoker	0.5	4
Asb-0496	73	Male	No	No	No	No	pneumonia	Direct	39	Unknown	Former Smoker	0.3	10
Asb-1442	70	Male	No	No	No	No	No	Indirect	16	Unknown	Former Smoker	1	40
Asb-0213	62	Male	Yes	Yes	No	No	No	Direct	30	Unknown	Never		
Asb-0846	82	Male	No	No	No	No	No	Direct	39	Unknown	Former Smoker	1	35
Asb-1386	69	Male	No	Yes	Yes	Yes	Atrial fibrillation, arthritis	Direct	2	Chrysotile	Former Smoker	1	20

Table 3
. Clinical features of patients with malignant pleural mesothelioma.

Patient ID	Age	Sex	Side	Mesotype	Resectable Tumor	Lymph Node Metastasis	Distant Metastasis	Stage	PET (SUV)
MPM 03	78	female	right	epithelioid	no	yes	no	III	n/a
MPM 06	66	female	right	epithelioid	no	no	no	III	6
MPM 07	73	male	right	sarcomatoid	no	no	no	II	11.1
MPM 08	70	male	left	epithelioid	no	no	no	II	n/a
MPM 09	55	female	right	biphasic	no	yes	no	III	n/a
MPM 12	67	male	right	desmoplastic	no	yes	contralateral lung	IV	n/a
MPM 13	71	male	left	epithelioid	no	no	contralateral lung	IV	n/a
MPM 15	79	male	left	biphasic	no	yes	no	III	n/a
MPM 21	72	female	left	biphasic	yes	yes	no	III	18.4
MPM 23	72	male	left	epithelioid	no	no	no	III	8.9
MPM 24	70	male	right	epithelioid	no	yes	no	III	13.7
MPM 25	81	male	right	epithelioid	yes	no	no	II	13.4
MPM 27	57	male	right	epithelioid	no	no	no	IV	5.3
MPM 28	76	male	right	epithelioid	no	no	peritoneal	IV	n/a
MPM 29	80	male	right	epithelioid	no	no	peritoneal	IV	n/a
MPM 31	75	male	right	epithelioid	no	no	no	III	n/a
MPM 32	76	male	right	epithelioid	no	yes	no	III	5.1
MPM 33	79	male	right	epithelioid	no	no	no	II	4.2
MPM 34	68	male	right	biphasic	no	no	no	III	n/a
MPM 35	73	female	right	biphasic	no	no	no	II	8.5
MPM 37	82	male	right	epithelioid	no	no	no	I	n/a
MPM 40	72	male	left	epithelioid	yes	no	no	n/a	n/a
MPM 41	79	male	right	epithelioid	yes	no	no	II	3.7

2.8. Fluorescent verification of mesothelin expression

To verify the MSLN expression in each zone on the MesoFind chip, 50,000 RN5 cells were loaded, captured with anti-MSLN conjugated to magnetic microbeads, and washed following the same protocol stated earlier. Cells were then stained with anti-rabbit IgG conjugated to Alexa Fluor® 647 (ab150075, Abcam, Canada) and washed on-chip. MesoFind chips were then analyzed with fluorescent microscopy. The fluorescent intensities of 10 randomly selected cells from each zone were background-subtracted and normalized to the average fluorescent intensity at zone 1. The intensity values were then compared to predicted mesothelin expressions based on the average flow velocity in each zone.

2.9. Flow cytometry

Flow cytometry was used to detect the expression of mesothelin, CD34, and CD90. RN5, H2052, and H2452 were harvested from culture and prepared in PBS at 2×10^6 cells/mL. The cells were then incubated in 1% BSA in PBS for 30 minutes on ice. The samples were incubated at room temperature for 30 minutes in a 1% BSA in PBS buffer solution containing 2% (v/v) of anti-mesothelin biotin (ABIN2584767, Antibodies-Online, USA) for RN5 cells or 2% (v/v) of anti-mesothelin biotin (BS-0300R-BIOTIN, Bioss Antibodies, USA) for H2052 and H2452 cells. The samples were then washed three times with 0.1% Tween-20 and 1% BSA in PBS. Afterwards, cells were then incubated in the dark for 1 hour at room temperature with a cocktail of antibodies containing either 2mg/mL of anti-CD34 AF488 (bs-8996R-A488, Bioss Antibodies, USA), 2mg/mL of anti-CD90 AF555 (bs-0778R-A555, Bioss Antibodies, USA), and 2 mg/mL streptavidin AF647 (405237, Biolegend, USA) for RN5 samples or 1mg/mL of anti-CD34 AF488 (ab195013, Abcam, Canada), 0.5mg/mL of anti-CD90 AF555 (bs-10430R-A555, Bioss Antibodies, USA), and 2 mg/mL streptavidin AF647 (405237, Biolegend, USA) for H2052 and H2452 samples. After washing three times with 0.1% Tween-20 and 1% BSA in PBS, the cells analyzed using the FACSCanto flow cytometer (BD Biosciences, USA) and 10,000 events were measured. Mice lavage samples were processed using the same protocol as RN5 samples.

2.10. Statistical analysis

All statistics were reported as mean ± SEM. Comparative groups were evaluated using unpaired t-test with $\alpha = 0.05$. To determine the analytical sensitivity of the device, the capture efficiency of the MesoFind device was determined by introducing RN5, H2052, and H2452 cells into the chip and the proportion of MSLN+ cells captured on-chip were reported as capture efficiency (supplementary figure 1). A cut off expression index value was determined between comparative groups to maximize the geometric mean of clinical sensitivity and specificity. Clinical sensitivity and specificity were calculated as followed:

$$\text{Sensitivity} = \frac{True\ Positive}{True\ positive\ +\ False\ Negative}$$

$$\text{Specificity} = \frac{True\ Negative}{True\ Negative\ +\ False\ Positive}$$

True positive are outcomes that are above the set cut-off threshold and clinically evaluated as positive. In general, clinical sensitivity reports the proportion of correctly identified true positive values whereas the specificity reports the proportion of correctly identified true negative values.

2.11. Role of funding source

The funding source has no role in study design; in the collection, analysis, and interpretation of data; in the writing of the report; and in the decision to submit the paper for publication. No payment was received to write this article by a pharmaceutical company or other agency.

3. Results

3.1. MPC liquid biopsy approach

The microfluidic chip employed for MPC analysis utilizes immunomagnetic separation of mesothelin-expressing cells through nanoparticle-mediated cell sorting. Mesothelin is a generally accepted hallmark biomarker that is overexpressed in

epithelioid mesothelioma [30–32] while also a key biomarker presented on MPCs. This approach allows for simple sample preparation and analysis of whole unprocessed blood (Fig. 1A). Blood samples were initially labeled with anti-MSLN antibody conjugated to biotin. The samples were then incubated with anti-biotin antibodies functionalized to magnetic nanoparticles. Cells with high surface mesothelin expressions will generally have greater magnetic susceptibility. Cells are then loaded into the microfluidic device under the influence of an external magnetic field to facilitate the capture of MSLN+ cells. Embedded within the chip are numerous X-shaped microstructures to create low-flow regions to enhance the capture of target cells.

Due to the large degree of heterogeneity in mesothelioma, we anticipated the existence of heterogeneous subpopulations of MPC with variable expression of MSLN+, CD34+, and CD90+ in circulation (Fig. 1B). To address this challenge, our microfluidic approach stratifies the target cells into 8 different capture zones, each corresponds to a specific expression level of cell-surface mesothelin (Fig. 1C). The channel heights increase between each consecutive zone leading to a stepwise decrease in flow velocity along the chip. As a result, cells with higher levels of magnetic labeling are captured in earlier zones under high flow velocity and correspondingly have higher mesothelin surface expression. Using this approach, we can generate a mesothelin expression profile by enumerating the cells distributed among the eight zones. To evaluate the identity of each MSLN+ cell, we have designed our chip to be compatible with immunofluorescence microscopy. For simplicity, we distinguish the variable CD34 and CD90-expressing MPC through the presence or absence of signal under immunofluorescent imaging. Hence, the contributing MPC subpopulations for our analysis are segregated based on following phenotypes: MSLN+ CD34+ CD90+, MSLN+ CD34- CD90+, MSLN+ CD34+ CD90-, MSLN+ CD34+, and MSLN+ CD90+.

Although the shedding of mesothelin in the blood has been widely accepted to correlate with mesothelioma progression once the tumor reaches a certain volume [18-21], it is unclear whether this elevation in mesothelin shedding occurs through the elevation of mesothelin protein expression on single cells or via the cumulative increase in the number of mesothelin-expressing cells. Regardless of the mechanism, we can calculate a single expression index value that encompasses both criteria through the following equation:

$$\text{Expression Index (EI)} = \sum_{n=1}^{8} (N_n \text{ x } V_n)$$

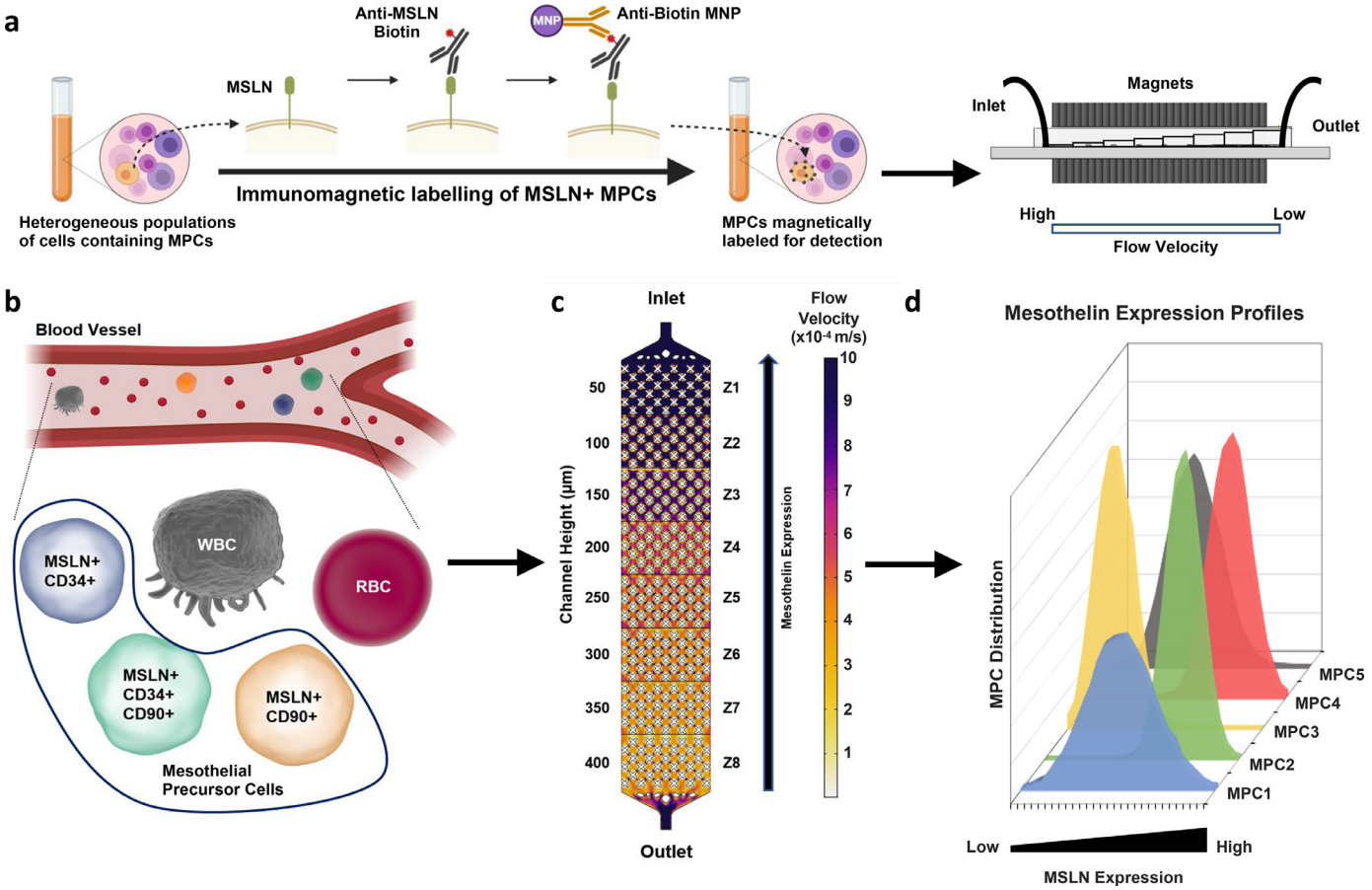

Fig. 1. Overview of mesothelial precursor cells (MPC) analysis using a microfluidic approach. (a) Sample preparation for MPC analysis is quick and simple. MSLN+ cells are tagged with biotinylated anti-MSLN antibody and further conjugated with anti-biotin magnetic nanoparticle (MNP) complex. Magnetically labeled samples are loaded into the microfluidic chip at 500μL/h with external magnets placed above and below the device to facilitate magnetic trapping of targeted cells. (b) Multiple populations of MPC exist in circulation and are subcategorized based on varying combinations of CD34 and/or CD90 in conjunction with mesothelin (MSLN). Image created with BioRender. (c) Overview of MesoFind microfluidic chip for MPC isolation. The microfluidic device contains 8 different zones with a sequential increase in height from 50μm to 400μm (inlet-to-outlet) and features varying average linear flow velocities (1.0x, 0.50x, 0.33x, 0.25x, 0.20x, 0.17x, 0.14x, 0.13x). Cells magnetically labeled with mesothelin are captured in different zones based on the relative amount of magnetic content. Cells with higher MSLN expression (high magnetic content) are captured in earlier zones whereas cells with less MSLN (low magnetic content) are captured in later zones. Captured cells are fluorescently labeled with CD34 and CD90 antibodies to identify and isolate different MPC subpopulations. (d) MSLN expression profiles are generated for each MPC subpopulation based on the captured location on the chip. Each MPC subtypes are predicted to exhibit different clinical characteristics in patients and their expression of MSLN correlates to the severity of the conditions.

where N_n represents the number of target cells captured in zone n, and V_n is the relative flow velocity which corresponds to the level of mesothelin surface protein expression per cell. The V_n for the zone closest to the outlet (lowest expression) was given an arbitrary value of 1 (i.e. $V_8 = 1$) and the V_n for the remaining zones were normalized to this value. Generally, the higher the EI, the higher the expression of mesothelin. With this approach, we can utilize the mesothelin EI to generate a threshold value for diagnostic purposes while also cross-correlating between various clinical characteristics for prognostic evaluation in mesothelioma patients (Fig. 1D). The MesoFind assay allows for the simultaneous analysis of multiple populations of cells and thus allows us to better understand the contributing roles of each MPC subpopulation in mesothelioma development.

3.2. Validation in murine models

To ensure optimal capture of MPCs, the processing flow rate was carefully adjusted to allow for the complete capture of low-mesothelin expressing cells while maintaining high throughput and adequate distribution along the device. This optimal threshold was reached at 0.5mL/h, where the total recovery was maximized in mouse mesothelioma cells lines (RN5 104 ± 6%) and human mesothelioma cell lines (H2052 97 ± 2%, H2452 98 ± 6%) spiked in healthy human blood (Fig. 2A). To distinguish between MPC subpopulations and leukocytes, we performed immunofluorescent staining with DAPI, CD34 (AF488), CD90 (AF555), and CD45 (APC) on-chip. Cells were identified with DAPI nuclear stain while leukocytes were negatively selected with CD45+ staining. Three subpopulations of MPC shown in Fig. 2B were clearly differentiated using fluorescence imaging and represented as MSLN+ CD34+ CD90+ CD45-, MSLN+ CD34- CD90+ CD45-, and MSLN+ CD34+ CD90- CD45-.

We first evaluated the capability of the MesoFind chip to detect traditional MPC cells (MSLN+ CD90+ CD45+). RN5 mouse mesothelioma cell lines were injected intraperitoneally in mice and sacrificed after 1 – 6 weeks. We collected both blood and peritoneal lavage samples and compared the performance of flow cytometry and MesoFind for MPC detection (Fig. 2C). The increasing number of MPCs in mice peritoneal lavage was similarly detected using MesoFind (Fig. 2D) and flow cytometry (Fig. 2E) due to the abundance of MPCs in the peritoneal cavity. On the other hand, we were only able to

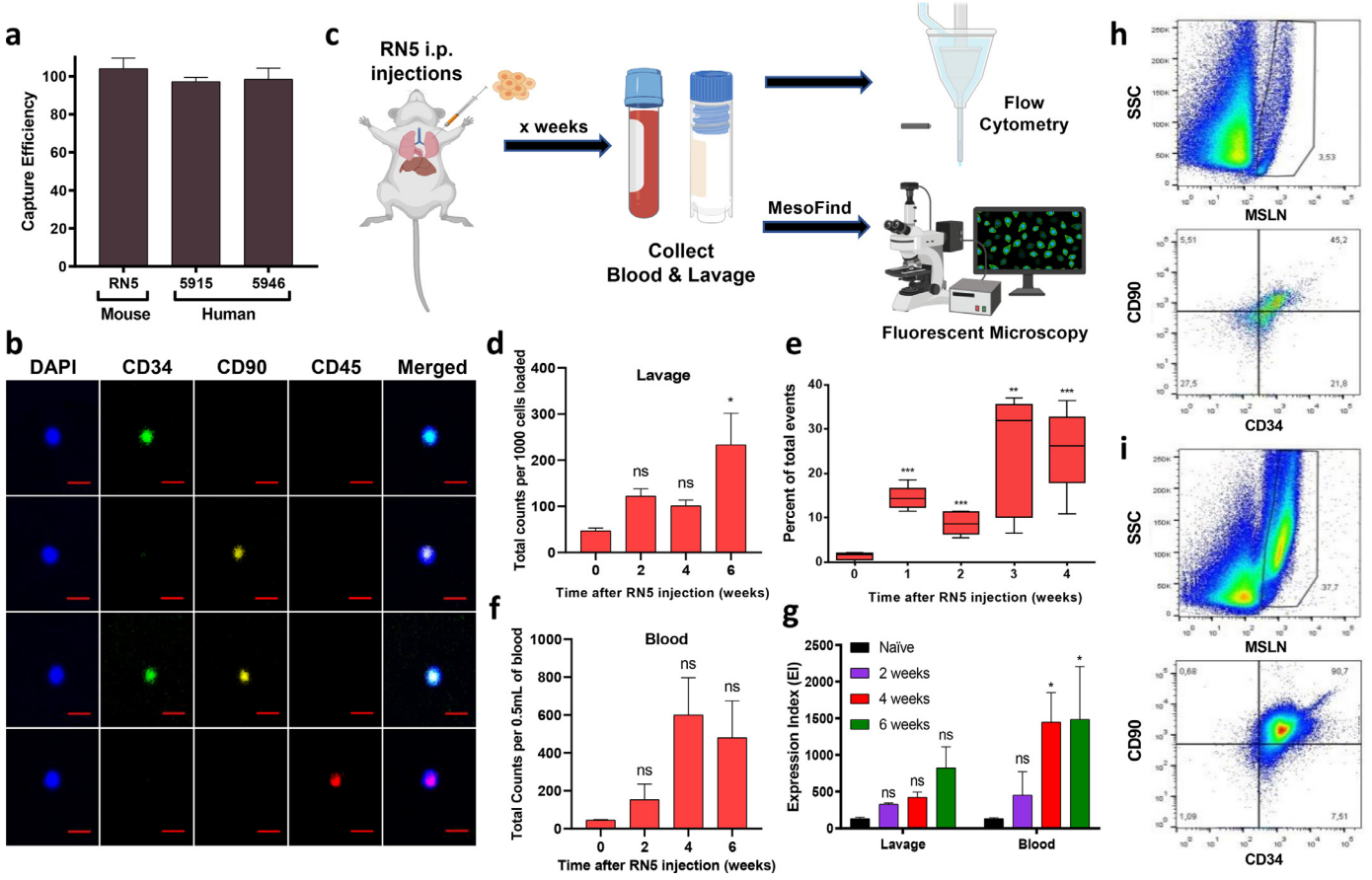

Fig. 2. Validation of the microfluidic approach for MPC analysis. (a) Captured efficiency of mice mesothelioma cell line (RN5) and human mesothelioma cell lines (H2052 and H2452) spiked in healthy blood using MesoFind microfluidic chips. (b) Identification of different MPC and leukocytes from blood using fluorescence microscopy after cell entrapment using MesoFind devices. Three differing MPC subtypes (top three) shown here contains different combinations of CD34 and/or CD90 expression and were negative for CD45. Leukocytes shown express CD34- CD90- CD45+ but were generally identified as CD45+ and can have varying expressions of CD34 and CD90 (not shown). All scale bars are 20 um. (c) Schematic of mesothelioma mice model analysis. RN5 mesothelioma cells were injected intraperitoneally (i.p.) and mice were sacrificed between 1 to 6 weeks post-injection. Control mice were injected with saline. The lavage and blood collected from the mice were analyzed using flow cytometry or MesoFind microfluidic analysis followed by fluorescence microscopy for the identification of different MPC populations. Images were created with BioRender. (d) Total MSLN+ CD34+ CD90+ MPC captured from the lavage collected from mice using MesoFind analysis. A general increase in total counts observed from 0 to 6 weeks post-injection. (e) Flow cytometry of MSLN+ CD34+ CD90+ MPC in lavage samples. No significant change was observed after 4-weeks post-injection. No MPC were detected in blood samples using flow cytometric analysis (not shown). (f) Total MSLN+ CD34+ CD90+ MPC captured from the blood of mice using MesoFind analysis. A general increase in total counts observed from 0 to 6 weeks post-injection. (g) Mesothelin expression indices (EI) for MSLN+ CD34+ CD90+ MPC in lavage and blood samples from 0 to 6 weeks post-injection using MesoFind analysis. (h) Flow cytometric gating for MSLN+ cells and CD34+ CD90+ cells in naive mice and (i) 4 weeks RN5 post-injected mice. All analysis was performed in triplicates (n=3). Error bars for Fig. 2 d,f, and g represent standard error of mean. All reported values were compared to values at 0 week (d,e,f) or naïve mice (g) using unpaired t-test, $^{*}p<0.05$, $^{**}p<0.01$, $^{***}p<0.001$.

visualize MPCs in the blood using MesoFind (Fig. 2F, G). Flow cytometry could not detect MPCs in the blood at any time point during tumor progression and the naïve state despite using the same flow cytometric gating criteria that were used to detect the cells in the lavage (Fig. 2H, I). Furthermore, by evaluating EI instead of total counts, we observed a more noticeable correlation in mesothelin expression with respect to the progression of the disease (Fig. 2G). This suggests that the increase in the number of high-expressing mesothelin MPC is correlated to the advancement of mesothelioma.

3.3. Clinical evaluation of MPCs

We then proceeded to validate MesoFind using clinical specimens. This study consisted of 23 patients with MPM confirmed by histological diagnosis (MPM), 23 individuals with known exposure to asbestos (ASB), and 10 healthy donors (HD) with no known exposure to asbestos. The asbestos-exposed individuals were recruited from our screening program with low dose CT chest [46] and MPM patients were recruited from our mesothelioma clinic during their evaluation for surgical resection [47]. Overall, there was a noticeable increase in the total number of traditional MPCs (MSLN+ CD34+ CD90+ CD45-) in whole blood for the ASB and MPM group compared to healthy donors (Fig. 3A). It is interesting to note that circulating MPCs in the ASB group were elevated in some individuals despite the absence of known malignancy suggesting that individuals may have a different degree of severity in pleural damage after asbestos exposure and some may be at a higher risk for mesothelioma. We also observed, as expected, that MPC levels were particularly high in patients with epithelioid MPM compared to biphasic and sarcomatoid MPM. We further evaluated the EI of all MPC subpopulations (Fig. 3B) and analyzed each of them for their sensitivity and specificity in predicting various clinical conditions. The MPC subpopulations with the highest overall sensitivity and specificity are summarized in Fig. 3 C – H.

In terms of diagnostic value, all MPC subpopulations exhibited a significantly higher mesothelin expression in MPM patients

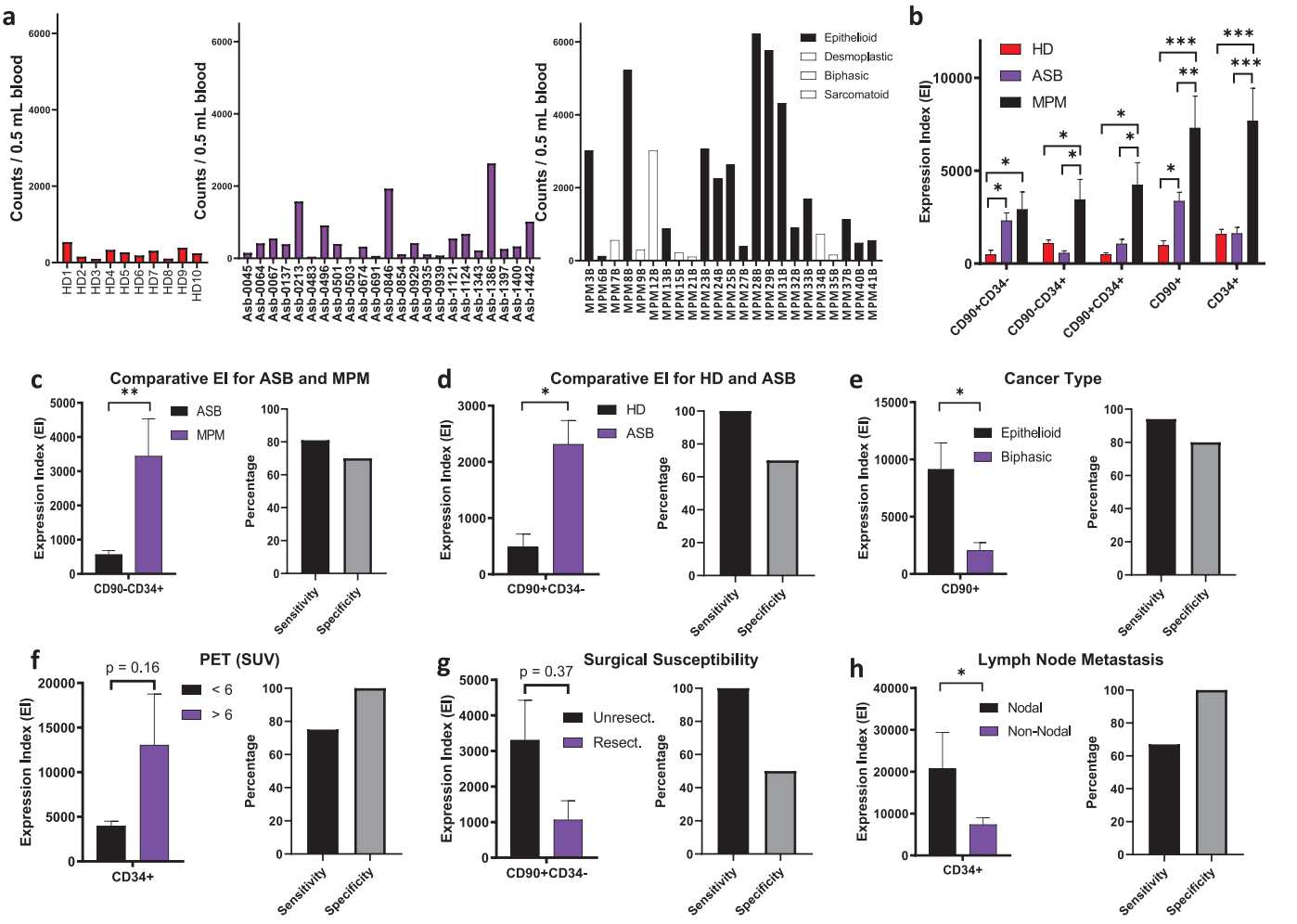

Fig. 3. Clinical utility of analyzing various MPC subpopulations using MesoFind device. (a) Total blood counts for MSLN+ CD34+ CD90+ MPC from healthy donor (HD, n=10), asbestos-exposed individuals (ASB, n=23), and malignant pleural mesothelioma patients (MPM, n=23) using MesoFind devices. (b) Comparison of mesothelin expression indices between varying subpopulations of MPC (CD90+ CD34-, CD90- CD34+, CD90+ CD34+, CD90+, CD34+) in HD, ASB, and MPM individuals. All MPC were MSLN+ and CD45-. (c-h) MSLN expression indices (EI) for most representative MPC subtypes in each clinical evaluation. Overall, higher MSLN expression indices corresponded to higher severity in clinical tests. EI cut-off values between each group were determined and the clinical sensitivity and specificity were reported (right). (c) EI of MSLN+ CD90- CD34+ CD45- MPC in ASB (n=23) and MPM (n=23). Cut-off EI=500. (d) EI of MSLN+ CD90+ CD34- CD45- MPC in HD (n=10) and ASB (n=23). Cut-off EI=200. (e) EI of MSLN+ CD90+ CD45- MPC were compared between epithelioid (n=16) and biphasic (n=5) cancer subtypes. Cut-off EI = 2650. (f) EI of MSLN+ CD34+ CD45- MPC in patients with low (<6) (n=4) and high (>6) (n=4) SUV scores through PET scans were compared. Cut-off EI=6700. (g) EI of MSLN+ CD90+ CD34- CD45- MPC for patients with unresectable tumors (n=19) and resectable tumors (n=4) were compared. Cut-off EI=200. (h) Presence (n=3) and absence (n=13) of lymph node metastasis was compared through MSLN+ CD34+ CD45- MPC. Cut-off EI=24500. Statistics are performed with unpaired t-tests, *$p<0.05$, **$p<0.01$, ***$p<0.001$.

compared to HD and thus can be used to reliably distinguish between healthy individuals and those with malignant disease (Fig. 3B). Additionally, we were interested in analyzing the ASB group more specifically as these individuals are at risk of developing mesothelioma, but the risk for a specific individual is unknown. Hence, MPC could be extremely helpful to refine screening in asbestos-exposed individuals to be able to focus on individuals at particularly high risk for mesothelioma.

After evaluating an EI threshold value for all subpopulations, the MPC subtype with MSLN+ CD90- CD34+ CD45- marker expression had the most distinct EI between ASB and MPM with a clinical sensitivity of 81% and specificity of 70% (Fig. 3C). This MPC subpopulation interestingly shows an elevation only in malignancy and therefore can complement as a screening tool to closely monitor ASB individuals at high risk for developing mesothelioma before malignancy is fully established. On the other hand, MSLN+ CD90+ CD34- CD45- MPC subpopulations elicit higher mesothelin response in ASB individuals compared to HD, which suggests the early involvement of these MPC subtypes in tissue repair and maintenance (Fig. 3D).

Prognosis of mesothelioma is often difficult to determine due to the heterogeneity of patients and poorly defined features for characterization. MesoFind can assist in the prognosis by providing clear and objective numerical scores. Here, we evaluated all the MPC subpopulations for different clinical prognosis. Mesothelioma is often categorized into different histological subtypes. While epithelioid subtypes are the most prevalent, sarcomatoid subtypes are often associated with worse prognosis and biphasic tumors are generally an intermediary between the two. In our study, we examined 16 individuals with epithelioid and 5 individuals with biphasic mesothelioma who had complete staging with a plan for possible radical surgery. The MPC subpopulation of MSLN+ CD90+ CD45- displayed a marked increase in mesothelin expression for epithelioid MPM compared to biphasic MPM (Fig. 3E). Although biphasic cancers tend to have a poorer prognosis, it nonetheless agrees with other reports as mesothelin tends to exhibit greater expressions in epithelioid cancer compare to other histotypes [48,49]. Using an EI threshold value of 2650, MesoFind has a high sensitivity (95%) and specificity (80%) for distinguishing between biphasic and epithelioid MPM subtypes. In accordance with these results, we shifted our focus on the analysis of epithelioid MPM as they are more prevalent in the mesothelioma population compared to other histotypes and more responsive to changes in mesothelin expression. Due to the low number of PET scans data (n=8), we divided the data into high and low standardized uptake values (SUV) (SUV >6 and SUV ≤ 6), which is known to be an adequate cut-off to determine prognosis [50]. MSLN+ CD34+ CD45- MPC subtype displayed the greatest separation between the two groups however the difference is only significant at an 84% confidence level ($p = 0.16$) (Fig. 3F). Although it is not intended to replace PET scans, MesoFind could provide another indirect measurement of tumor progression and growth with high sensitivity and specificity (84% and 87% respectively) (Fig. 3F).

Some MPM patients in this study had developed advanced stages of mesothelioma and as a result, many patients were not eligible for radical surgery. To evaluate the predictive potential of MPCs for tumor resectability, we performed a retrospective analysis of MPC populations on our MPM cohort. MSLN+ CD90+ CD34- CD45- subtypes had the greatest predictive value to determine resectability with a 100% sensitivity, confirming that MSLN+ CD90+ CD34- CD45- tends to be associated with earlier stage MPM (Fig. 3G). However, the number of patients undergoing surgery in this cohort was small and the average EI between resectable and unresectable tumors was not significant ($p = 0.38$) with only 50% specificity obtained using an EI cut-off value of 200. Nodal metastasis is another important prognostic factor in MPM that can be difficult to determine clinically [51]. The EI values for MSLN+ CD34+ CD45- populations were significantly different between individuals with and without nodal metastasis (Fig. 3H). With a cut-off EI value of 24500, this MPC population can assist with screening for nodal metastasis in MPM with a clinical sensitivity and specificity of 67% and 100% respectively. Overall, these findings demonstrate that circulating MSLN+ CD90+ CD45- MPC subtype increases with pleural damage related to asbestos and continues to rise during the early development of mesothelioma, while MSLN+ CD34+ CD45- MPC subtype starts rising with established MPM and are associated with more advanced mesothelioma (Fig. 4).

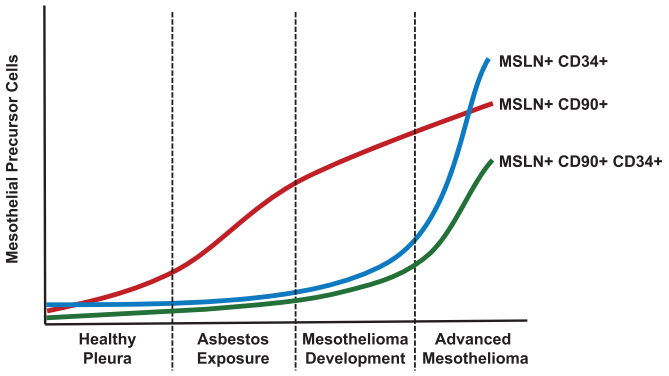

Fig. 4. Summary of MPC subtypes through different stages leading to mesothelioma.

4. Discussion

In this study, we have developed an assay that effectively identifies various MPC populations and we have highlighted the clinical potential in evaluating circulating MPC in mesothelioma and asbestos-exposed individuals. For this study, other causes of mesothelial inflammation such as pleural infection and pleurodesis were not included and could be a potential source of false positive counts of MPCs. MPCs are still largely understudied due to the difficulty in their detection, particularly in the blood. Unlike CTCs, MPCs can be elevated well before tumor development as shown in our study. We were able to detect 262 ± 43, 537 ± 137, and 1664 ± 360 MPCs in 0.5mL of blood from HD, ASB, and MPM patients respectively. In contrast, for 7.5mL of blood CTCs are detected on the order of 1 CTCs for healthy and benign diseases and up to the order of 10 CTCs for malignant diseases using CellSearch [52]. From a biological perspective, CTCs are often able to disseminate into the blood after significant development in the tumor. MPCs on the other hand are predicted to mobilize as soon as inflammation occurs in the mesothelium. As such, MPCs are expected to be elevated much earlier compared to CTCs in mesothelioma.

Using MesoFind, we have elucidated key MPC subtypes with excellent diagnostic and prognostic potential. All subtypes of MPC were significantly elevated compared to healthy donors with no known exposure to asbestos. Two MPC subtypes, MSLN+ CD90+ CD34- CD45- and MSLN+ CD90- CD34+ CD45-, had a different profile in the blood depending on the exposure to asbestos and presence of advanced mesothelioma. MSLN+ CD90+ CD34- CD45- exhibited a much greater level of mesothelin in asbestos-exposed individuals compared to healthy controls, even before malignancy. The importance of CD90 in chronic pleural damage is supported by previous work demonstrating that CD90 expression is critical for the recruitment of leukocytes to the site of inflammation [53]. These findings suggest that CD90+ MPC have an early role in the recruitment of inflammatory cells after pleural damage. Future prospective studies on these populations will be important to clarify the clinical roles of MPC in early stages of MPM development and provide more evidence on the early diagnostic and staging utility of MPC. The role of MPC in the context of mesothelioma in situ will also be an important area of investigations. In contrast, MSLN+ CD90- CD34+ CD45- are more

relevant in the context of mesothelioma since this MPC subtype is extremely low in the absence of mesothelioma despite asbestos exposure, but significantly elevated in MPM and associated with markers of advanced disease characterized by high SUV on PET scan and lymph node metastasis on biopsy. It is not clear whether the CD34+ MPC subtypes are contributing to disease progression or simply a bystander related to malignancy. MSLN+ CD90- CD34+ CD45- MPC subtype could potentially be helpful to monitor tumor response after therapeutic interventions and act as a predictive marker for cancer progression or recurrence. Surgical resection was predominantly performed in patients with high MSLN+ CD90+ and low MSLN+ CD34 +subpopulations (Fig. 3G), suggesting that the balance between these two subtypes of MPC may help to detect MPM at an early stage accessible to surgery.

We have also demonstrated the merits of using MesoFind for the analysis of MPC in blood. Compared to flow cytometry, our approach has much greater sensitivity and requires less sample volume for analysis. We have also evaluated the MSLN expression in each zone through analyzing fluorescent intensities (supplementary figure 2). Although the fluorescent signals correlated strongly with predicted mesothelin expression values in early zones (zones 1 to 4), the fluorescent resolution falls off after around zone 5 and is unable to distinguish MSLN expression in later zones. In addition, fluorescent intensities signals are difficult to standardize due to complications such as large variation between microscopes and varying interference from stray light. Overall, the MSLN expression MesoFind assay is much easier to standardize and has a higher resolution compared to evaluating fluorescent intensities alone. The MesoFind assay also maintains the ability to segregate heterogeneous populations of cells and allow for the phenotypic profiling of surface markers. Segregated populations can be isolated from the chip for further genetic analysis and can complement other genetic detection tools such as RNA editing quantification [54].

The capability to process whole blood with simple workflow highlights the amenability of using this technique in clinical practice. Although the total run time for the MesoFind assay is approximately 6 hours, the microfluidic assay, fluorescent scanning, and image analysis can all be fully automated. The material cost comes to around $4 USD per device but with injection molding, the costs can be further reduced. Overall, the MesoFind assay is inexpensive and simple to use making it very feasible for clinical adoption.

In conclusion, our microfluidic assay successfully addressed many clinical implications of detecting and identifying heterogeneous populations of MPC. Through the evaluation of both murine and clinical samples, we have consistently identified higher expressions of MPC as a function of disease progression. In our cohort of 23 MPM, 23 ASB, and 10 HD, we were able to identify specific subtypes of MPC that have excellent predictive values for clinical diagnosis and prognosis of mesothelioma. This is the first study analyzing the involvement of MPC in mesothelioma and thus further investigations will be important to elucidate the biological mechanism and clinical roles of MPC in mesothelioma progression. To ensure the practical usage of this technology, prospective studies that monitors MPC in patients through disease development and therapeutic intervention will help to provide the evidence for the possible integration of this technology in a clinical setting.

Declaration of Competing Interests

Dr. Shana O. Kelley reports grants from Cellular Analytics, outside the submitted work. In addition, Dr. Shana O. Kelley has a patent “Device for capture of particles in a flow” US10073079 licensed to Cellular Analytics. Dr Marc de Perrot received personal fees from Astra-Zeneca and Bayer outside of the submitted work. None of the other authors has anything to disclose.

Data Sharing

Deidentified participant data will be accessible with a signed data access agreement upon approval of a proposal for 36 months following article publication.

Acknowledgments

This study was supported by Princess Margaret Hospital Foundation Mesothelioma Research Fund, Toronto General & Western Hospital Foundation.

Supplementary materials

Supplementary material associated with this article can be found, in the online version, at doi:10.1016/j.ebiom.2020.103031.

References

[1] Scherpereel A, Wallyn F, Albelda SM, Munck C. Novel therapies for malignant pleural mesothelioma. Lancet Oncol 2018;19:e161–72.
[2] Mutti L, Peikert T, Robinson BWS, et al. Scientific advances and new frontiers in mesothelioma therapeutics. J Thorac Oncol 2018;13:1269–83.
[3] Zhang W, Wu X, Wu L, Zhang W, Zhao X. Advances in the diagnosis, treatment and prognosis of malignant pleural mesothelioma. Ann Transl Med 2015;3:1–8.
[4] Murphy DJ, Gill RR. Overview of treatment related complications in malignant pleural mesothelioma. Ann Transl Med 2017;5. doi: 10.21037/atm.2017.03.97.
[5] Carbone M, Adusumilli PS, Alexander HR, et al. Mesothelioma: scientific clues for prevention, diagnosis, and therapy. CA Cancer J Clin 2019;69:402–29.
[6] Wang S, Ma K, Wang Q, et al. The revised staging system for malignant pleural mesothelioma based on surveillance, epidemiology, and end results database. Int J Surg 2017;48:92–8.
[7] Armato SG, Blyth KG, Keating JJ, et al. Imaging in pleural mesothelioma: A review of the 13th International Conference of the International Mesothelioma Interest Group. Lung Cancer 2016;101:48–58.
[8] Arnold DT, Maskell NA. Biomarkers in mesothelioma. Ann Clin Biochem 2018;55:49–58.
[9] Cristaudo A, Bonotti A, Simonini S, et al. Combined serum mesothelin and plasma osteopontin measurements in malignant pleural mesothelioma. J Thorac Oncol 2011;6:1587–93.
[10] Amati M, Tomasetti M, Scartozzi M, et al. Profiling tumor-associated markers for early detection of malignant mesothelioma: an epidemiologic study. Cancer Epidemiol Biomarkers Prev 2008;17:163–70.
[11] Schneider J, Hoffmann H, Dienemann H, Herth FJF, Meister M, Muley T. Diagnostic and prognostic value of soluble mesothelin-related proteins in patients with malignant pleural mesothelioma in comparison with benign asbestosis and lung cancer. J Thorac Oncol 2008;3:1317–24.
[12] Robinson BWS, Creaney J, Lake R, et al. Mesothelin-family proteins and diagnosis of mesothelioma. Lancet 2003;362:1612–6.
[13] Ren R, Yin P, Zhang Y, et al. Diagnostic value of fibulin-3 for malignant pleural mesothelioma: a systematic review and meta-analysis. Oncotarget 2016;7:84851–9.
[14] Pei D, Li Y, Liu X, et al. Diagnostic and prognostic utilities of humoral fibulin-3 in malignant pleural mesothelioma: Evidence from a meta-analysis. Oncotarget 2017;8:13030–8.
[15] Pass HI, Levin SM, Harbut MR, et al. Fibulin-3 as a blood and effusion biomarker for pleural mesothelioma. N Engl J Med 2012;367:1417–27.
[16] Pass HI, Lott D, Lonardo F, et al. Asbestos exposure, pleural mesothelioma, and serum osteopontin levels. N Engl J Med 2005;353:1564–73.
[17] Ledda C, Senia P, Rapisarda V. Biomarkers for early diagnosis and prognosis of malignant pleural mesothelioma: The quest goes on. Cancers (Basel) 2018;10. doi: 10.3390/cancers10060203.
[18] Arnold DT, De Fonseka D, Hamilton FW, Rahman NM, Maskell NA. Prognostication and monitoring of mesothelioma using biomarkers: a systematic review. Br J Cancer 2017;116:731–41.
[19] Gillezeau CN, Van Gerwen M, Ramos J, Liu B, Flores R, Taioli E. Biomarkers for malignant pleural mesothelioma: a meta-analysis. Carcinogenesis 2019;40:1320–31.
[20] Sun HH, Vaynblat A, Pass HI. Diagnosis and prognosis-review of biomarkers for mesothelioma. Ann Transl Med 2017;5:1–8.
[21] Liu H, Wu L, Ji K, Wang W. Prognostic value of several biomarkers for the patients with malignant pleural mesothelioma. Tumor Biol 2015;36:7375–84.
[22] Tolani B, Acevedo LA, Hoang NT, He B. Heterogeneous contributing factors in MPM disease development and progression: Biological advances and clinical implications. Int J Mol Sci 2018;19:1–23.
[23] Mapara MY, Sykes M. Tolerance and cancer: mechanisms of tumor evasion and strategies for breaking tolerance. J Clin Oncol 2004;22:1136–51.
[24] Moalli PA, MacDonald JL, Goodglick LA, Kane AB. Acute injury and regeneration of the mesothelium in response to asbestos fibers. Am J Pathol 1987;128:426–45.

[25] Khanna S, Thomas A, Abate-Daga D, et al. Malignant mesothelioma effusions are infiltrated by CD3+ T cells highly expressing PD-L1 and the PD-L1+ tumor cells within these effusions are susceptible to ADCC by the anti-PD-L1 antibody avelumab. J Thorac Oncol 2016;11:1993–2005.
[26] Wu L, Yun Z, Tagawa T, Rey-McIntyre K, Anraku M, De Perrot M. Tumor cell repopulation between cycles of chemotherapy is inhibited by regulatory T-cell depletion in a murine mesothelioma model. J Thorac Oncol 2011;6:1578–86.
[27] Banchereau J, Palucka AK. Dendritic cells as therapeutic vaccines against cancer. Nat. Rev. Immunol. 2005;5:296–306.
[28] Gabrilovich DI, Nagaraj S. Myeloid-derived suppressor cells as regulators of the immune system. Nat. Rev. Immunol. 2009;9:162–74.
[29] Jinushi M, Chiba S, Yoshiyama H, et al. Tumor-associated macrophages regulate tumorigenicity and anticancer drug responses of cancer stem/initiating cells. Proc Natl Acad Sci U S A 2011;108:12425–30.
[30] Rehrauer H, Wu L, Blum W, et al. How asbestos drives the tissue towards tumors: YAP activation, macrophage and mesothelial precursor recruitment, RNA editing, and somatic mutations. Oncogene 2018;37:2645–59.
[31] Rinkevich Y, Mori T, Sahoo D, Xu PX, Bermingham JR, Weissman IL. Identification and prospective isolation of a mesothelial precursor lineage giving rise to smooth muscle cells and fibroblasts for mammalian internal organs, and their vasculature. Nat Cell Biol 2012;14:1251–60.
[32] Carmona R, Cano E, Grueso E, et al. Peritoneal repairing cells: A type of bone marrow derived progenitor cells involved in mesothelial regeneration. J Cell Mol Med 2011;15:1200–9.
[33] Chen Y, Li P, Huang PH, et al. Rare cell isolation and analysis in microfluidics. Lab Chip. 2014;14:626–45.
[34] Poudineh M, Sargent EH, Kelley SO. Amplified Micromagnetic Field Gradients Enable High-Resolution Profiling of Rare Cell Subpopulations. ACS Appl Mater Interfaces 2017;9:25683–90.
[35] Labib M, Green B, Mohamadi RM, et al. Aptamer and antisense-mediated two-dimensional isolation of specific cancer cell subpopulations. J Am Chem Soc 2016;138:2476–9.
[36] Poudineh M, Aldridge PM, Ahmed S, et al. Tracking the dynamics of circulating tumour cell phenotypes using nanoparticle-mediated magnetic ranking. Nat Nanotechnol 2017;12:274–81.
[37] Wang Z, Gagliardi M, Mohamadi R, et al. Ultrasensitive and rapid quantification of cardiomyocyte populations rare tumorigenic stem cell. Sci Adv 2020;6 aay7629.
[38] Kermanshah L, Poudineh M, Ahmed S, et al. Dynamic CTC phenotypes in metastatic prostate cancer models visualized using magnetic ranking cytometry. Lab Chip 2018;18:2055–64.
[39] Mair B, Aldridge PM, Atwal RS, et al. High-throughput genome-wide phenotypic screening via immunomagnetic cell sorting. Nat Biomed Eng 2019;3:796–805.
[40] Green BJ, Kermanshah L, Labib M, et al. Isolation of phenotypically distinct cancer cells using nanoparticle-mediated sorting. ACS Appl Mater Interfaces 2017;9:20435–43.
[41] Nemr CR, Smith SJ, Liu W, et al. Nanoparticle-mediated capture and electrochemical detection of methicillin-resistant staphylococcus aureus. Anal Chem 2019. doi: 10.1021/acs.analchem.8b04792.
[42] Green BJ, Nguyen V, Atenafu E, et al. Phenotypic profiling of circulating tumor cells in metastatic prostate cancer patients using nanoparticle-mediated ranking. Anal Chem 2019;91:9348–55.
[43] Aldridge PM, Mukhopadhyay M, Ahmed SU, et al. Prismatic deflection of live tumor cells and cell clusters. ACS Nano 2018;12:12692–700.
[44] Poudineh M, Labib M, Ahmed S, et al. Profiling functional and biochemical phenotypes of circulating tumor cells using a two-dimensional sorting device. Angew Chemie - Int Ed 2017;56:163–8.
[45] Labib M, Mohamadi RM, Poudineh M, et al. Single-cell mRNA cytometry via sequence-specific nanoparticle clustering and trapping. Nat Chem 2018;10:489–95.
[46] Roberts HC, Patsios DA, Paul NS, et al. Screening for malignant pleural mesothelioma and lung cancer in individuals with a history of asbestos exposure. J Thorac Oncol 2009;4:620–8.
[47] Cho BCJ, Feld R, Leighl N, et al. A feasibility study evaluating surgery for mesothelioma after radiation therapy: the 'SMART' approach for resectable malignant pleural mesothelioma. J Thorac Oncol 2014;9:397–402.
[48] Ordóñez NG. Value of mesothelin immunostaining in the diagnosis of mesothelioma. Mod Pathol 2003;16:192–7.
[49] Inaguma S, Wang Z, Lasota J, et al. Comprehensive immunohistochemical study of mesothelin (MSLN) using different monoclonal antibodies 5B2 and MN-1 in 1562 tumors with evaluation of its prognostic value in malignant pleural mesothelioma. Oncotarget 2017;8:26744–54.
[50] Bénard F, Sterman D, Smith RJ, Kaiser LR, Albelda SM, Alavi A. Prognostic value of FDG PET imaging in malignant pleural mesothelioma. J Nucl Med 1999;40:1241–5.
[51] Pass H, Giroux D, Kennedy C, et al. The IASLC mesothelioma staging project: improving staging of a rare disease through international participation. J Thorac Oncol 2016;11:2082–8.
[52] Miller MC, Doyle G V, Terstappen LWMM. Significance of circulating tumor cells detected by the cellsearch system in patients with metastatic breast colorectal and prostate cancer. J Oncol 2010;2010. doi: 10.1155/2010/617421.
[53] Schubert K, Polte T, Bönisch U, et al. Thy-1 (CD90) regulates the extravasation of leukocytes during inflammation. Eur J Immunol 2011;41:645–56.
[54] Crews LA, Jiang Q, Zipeto MA, et al. An RNA editing fingerprint of cancer stem cell reprogramming. J Transl Med 2015;13:52.